Cerebral Cortex June 2015;25:1676–1684
doi:10.1093/cercor/bht425
Advance Access publication January 12, 2014

Imaging Patterns of Brain Development and their Relationship to Cognition

Guray Erus[1], Harsha Battapady[1], Theodore D. Satterthwaite[1,2], Hakon Hakonarson[3], Raquel E. Gur[2], Christos Davatzikos[1] and Ruben C. Gur[2]

[1]Section of Biomedical Image Analysis, Department of Radiology, and Center for Biomedical Image Computing and Analytics, [2]Department of Psychiatry, University of Pennsylvania, Philadelphia, PA 19104, USA and [3]Center for Applied Genomics, Children's Hospital of Philadelphia, Philadelphia, PA 19104, USA

Address correspondence to Guray Erus, Department of Radiology, University of Pennsylvania, Philadelphia, PA 19104, USA. Email: guray.erus@uphs.upenn.edu

We present a brain development index (BDI) that concisely summarizes complex imaging patterns of structural brain maturation along a single dimension using a machine learning methodology. The brain was found to follow a remarkably consistent developmental trajectory in a sample of 621 subjects of ages 8–22 participating in the Philadelphia Neurodevelopmental Cohort, reflected by a cross-validated correlation coefficient between chronologic age and the BDI of $r = 0.89$. Critically, deviations from this trajectory related to cognitive performance. Specifically, subjects whose BDI was higher than their chronological age displayed significantly superior cognitive processing speed compared with subjects whose BDI was lower than their actual age. These results indicate that the multiparametric imaging patterns summarized by the BDI can accurately delineate trajectories of brain development and identify individuals with cognitive precocity or delay.

Keywords: age prediction, brain development index, DTI, MRI, SVR

Introduction

Healthy human brain maturation is a complex process evolving during childhood, adolescence, and young adulthood. Brain development involves dynamic processes of progressive and regressive changes that occur simultaneously in these periods (Silk and Wood 2011). While MRI lacks the resolution to characterize the cellular mechanism of the change in brain structures such as dendritic remodeling, cell death, synaptic pruning or myelination, advances in MRI technologies have provided valuable opportunities for studying structural brain measures and evaluate age effects in prospective samples of children and adolescents (Giedd et al. 1999; Gogtay et al. 2004; Sowell et al. 2004; Lenroot and Giedd 2006; Toga et al. 2006; Lenroot et al. 2007; Giedd and Rapoport 2010; Lebel and Beaulieu 2011; Ball et al. 2012). Several MRI studies revealed that white matter (WM) volume increases consistently throughout adolescence, whereas gray matter (GM) volume declines in a regionally heterogeneous pattern (Giedd et al. 1999; Toga et al. 2006; Ball et al. 2012).

More recently, diffusion tensor imaging (DTI) has been used for studying the microstructural properties of WM during development (Asato et al. 2010). Fractional anisotropy (FA) is a measure of the degree of anisotropy of the diffusion of water molecules in the brain. High FA suggests highly organized and myelinated fiber bundles. FA is used to quantify changes in evolving WM microstructure during development (Mukherjee et al. 2001; Barnea-Goraly et al. 2005; Ashtari et al. 2007; Asato et al. 2010). In contrast, the apparent coefficient of diffusion (ADC; or trace) is a measure of the freedom of diffusion, and declines in WM as FA increases in development. However, although DTI measures such as FA and ADC complement T_1-weighted images, few previous studies have attempted to integrate these 2 imaging modalities in the study of neurodevelopment.

Both cross-sectional (Barnea-Goraly et al. 2005; Toga et al. 2006; Lenroot et al. 2007; Asato et al. 2010) and longitudinal studies (Giedd et al. 1999; Gogtay et al. 2004; Sowell et al. 2004; Lenroot and Giedd 2006) have demonstrated that brain development is dynamic and spatially heterogeneous, with individual brain regions following temporally distinct maturational trajectories (Gogtay et al. 2004). In order to consider such complexity in an integrated fashion, recent studies (Dosenbach et al. 2010; Franke et al. 2010, 2012; Brown et al. 2012) have used multivariate machine-learning techniques to derive an amalgamated index of brain development. Specifically, T_1-weighted structural brain imaging can be used to predict an individual's chronologic age with a high degree of accuracy (subjects aged 19–86 years, $r = 0.92$, mean absolute error [MAE] = 5) (Franke et al. 2010, 2012). Similarly, Dosenbach et al. (2010) found that the complex patterns of functional connectivity can predict a subject's age during development, although with a somewhat lower degree of accuracy (subjects aged 7–30 years, $r^2 = 0.553$). Notably, however, only one prior study (Brown et al. 2012) has used more than one imaging modality to derive an integrated index of brain development, which successfully predicted the chronological age of subjects with very high accuracy (subjects aged 3–20, $r = 0.96$, MAE = 1.03).

This recent work has been valuable because it introduces the possibility of describing normative trajectories of brain development, akin to the growth charts used in pediatrics to screen for gross abnormalities of development. While such common measures such as height, weight, and head circumference (Nellhaus 1968) have proven to be of indisputable clinical utility, they are relatively insensitive to neuropsychiatric disorders, which are now increasingly conceptualized as developmental brain diseases (Paus et al. 2008; Insel 2009). Though prior studies have outlined normative trajectories of growth for individual brain regions across the lifespan (Giedd et al. 1999; Sowell et al. 2004; Ball et al. 2012), because of the multiplicity of brain regions and regional heterogeneity in developmental patterns, such data are difficult to integrate into clinical practice and are of limited clinical applicability considered in isolation. Conversely, techniques that distill multivariate patterns of brain development to a single dimension have the potential to be of practical utility.

While prior studies have demonstrated that multivariate patterns of brain images can accurately predict chronologic age, they have not examined whether deviations from this predicted

trajectory of development are related to individual differences in cognition. Establishing such a relationship is a prerequisite for demonstrating the putative utility of the approach; as a subject's age is a ground truth that is easily ascertained, if brain imaging patterns could predict subject age but did not relate to measures of brain function, such a technique would be of academic interest only. In contrast, as previously noted (Bunge and Whitaker 2012; Franke et al. 2012), if the degree to which a subject's estimated "brain age" diverged from their chronologic age was related to either precocity or delay of cognitive development, it would suggest that brain imaging may be a useful biomarker for the early detection of subtle developmental abnormalities.

We hypothesized that multimodal, multivariate patterns of brain maturation would relate to individual differences in maturation and cognition. Specifically, a support vector regression (SVR) procedure was used to derive an integrated brain development index (BDI) from T_1 and DTI images of children, adolescents, and young adults studied as part of the Philadelphia Neurodevelopmental Cohort (PNC). We validated the sensitivity of this index to the well-established sex difference in maturation, which is earlier in females (De Bellis et al. 2001; Lenroot et al. 2007), by applying the male predictors to the female sample and vice versa. With this procedure we tested the prediction that male-based models will underestimate chronological age in females while female-based scores will overestimate chronological age in males. We then identified a precocious and a delayed group and tested the prediction that individuals with a BDI that was higher than their chronologic age would demonstrate relative precocity in cognitive performance, whereas those with a BDI that was lower than their chronologic age would demonstrate signs of relative cognitive delay. As described below, results supported our hypotheses, providing novel evidence that individual differences in complex patterns of brain development have an impact on cognitive functioning.

Materials and Methods

Participants

Subjects were drawn from the PNC, a collaboration between the Brain Behavior Laboratory at the University of Pennsylvania (Penn) and the Center for Applied Genomics at Children's Hospital of Philadelphia (CHOP). Study procedures were reviewed and approved by the Institutional Review Boards of both Penn and CHOP. The population-based sample included youths who presented to the CHOP network for a pediatric visit and volunteered to participate in genomic studies of complex pediatric disorders (Gur et al. 2012). A subset of 1445 of these individuals received neuroimaging. The present results consider an interim subsample of the first 1078 subjects who participated in the study. Of these, 457 subjects were excluded for insufficient data quality ($n = 240$) or a history that suggested potential abnormalities of brain development ($n = 217$), such as history of medical problems that might affect brain function, a history of inpatient psychiatric hospitalization, or current use of psychotropic medication. The final sample included 621 subjects aged 8–22 years (351 female); mean age 15.08 years (3.27 standard deviation [SD]).

Computerized Neurocognitive Battery

As previously described (Gur et al. 2010 ,2012), the 1-h Penn Computerized Neurocognitive Battery (CNB) was administered to all participants, and consisted of 14 tests that evaluate a broad range of cognitive functions: abstraction and mental flexibility (ABF), attention (ATT), working memory (WM), verbal memory (VMEM), face memory (FMEM), spatial memory (SMEM), language reasoning (LAN), nonverbal reasoning (NVR), spatial processing (SPA), emotion identification (EMI), emotion differentiation (EMD), age differentiation (AGD), sensorimotor processing speed (SM), and motor speed (MOT). Except for the SM and MOT tests that only measure speed, each test provides measures of both accuracy and speed. For this developmental sample, instructions and vocabulary for verbal stimuli were simplified from the adult CNB. Cognitive assessment was completed during a separate session from neuroimaging; length of time between the 2 sessions averaged 3.4 months. As detailed in Gur et al. (2012) the assessment session was scheduled at home (68.8% of participants) or in the laboratory (31.2%), according to family and subject preference. During task administration, potential interference was minimized, standard instructions were read aloud in addition to appearing on the screen, and a professional testing environment was maintained. Tests were administered in a fixed order that was based on previous experience and designed to maintain participants' engagement in the tasks and prevent fatigue. Breaks were offered approximately every 15 min. Raw accuracy and speed scores were normalized by age within the entire cohort of the PNC study ($n = 9138$). Specifically, accuracy and speed for each test were z-transformed based on the mean and SD of participants within a 1-year-age bin. As prior (Gur et al. 2012), for ease of presentation, higher z-scores always reflect better performance; z-scores where higher numbers reflected poorer performance (i.e., response time) were multiplied by −1.

MR Image Acquisition

Imaging data were acquired using a Siemens Tim Trio (Erlangen, Germany) 3T scanner equipped with 40 mT/m gradients and 200 mT/m/s slew-rates. RF transmission utilized a quadrature body-coil and reception used a 32-channel head coil optimized for parallel imaging. The T_1-weighted protocol utilized a 3D, inversion-recovery, magnetization-prepared rapid acquisition gradient echo (MPRAGE) with TI/TR/TE = 1100/1810/3.51 ms, flip angle = 9°, matrix = 256 × 192, FOV = 240 × 180 mm, slices = 160, and slice thickness = 1 mm. DTI images were acquired with a twice-refocused spin-echo single-shot EPI sequence and a custom 64-direction diffusion set, with b-values of 0 and 1000 s/mm^2. The $b = 0$ scan was repeated 6 times, each $b = 1000$ scan was acquired once at each direction, for a total of 70 repetitions. The acquisition parameters were TR/TE = 8100/82 ms, matrix = 128 × 128, FOV = 240 mm, slices = 70, slice thickness = 2 mm and GRAPPA factor = 3.

Image Processing

The T_1 images were first preprocessed using an in-house automated pipeline, which included removal of extra-cranial material (skull-stripping) and cerebellum, bias correction, and tissue segmentation into GM, WM, and cerebrospinal fluid. Lateral ventricles (VN) were segmented by transferring manually segmented ventricle masks from a standard template to the subject space using the publicly available DRAMMS deformable registration tool (Ou et al. 2011). The quality of the initial and processed images were verified using strictly defined quality control procedures involving both automated and manual QA at each step of processing; images ($n = 240$) that failed QA procedures at any stage were removed from the analysis.

Images were registered prior to group-level analysis to a template that was the single most-representative T_1 image of the sample. The automated selection ensured that the template had the maximum overall similarity to all images in the dataset, measured by calculating the correlation ratio between each image pair after linear alignment. Regional volumetric maps, RAVENS (regional analysis of volumes examined in normalized space) maps (Goldszal et al. 1998; Davatzikos et al. 2001), were generated using the DRAMMS deformable registration package (Ou et al. 2011) to enable comparative analysis of tissue volumes on the common template space. The RAVENS approach has been extensively validated and applied in various studies (Resnick et al. 2000; Beresford et al. 2006; Gur et al. 2006; Driscoll et al. 2009). In this investigation, GM, WM, and ventricular (VN) RAVENS maps were generated, each quantifying the amount of respective tissue present in each brain region. The RAVENS maps were normalized by individual intracranial volume to adjust for global differences in intracranial size, down-sampled to 2 × 2 × 2 mm, and smoothed for

incorporation of neighborhood information using an 8-mm-diameter Gaussian filter.

Standard methods for calculating FA and ADC from the raw DTI images were used to derive voxel-wise maps (Le Bihan et al. 2001). FA and ADC maps from each subject were coregistered to the common template space by first aligning them linearly to the subject T_1 image and then applying the previously calculated deformation field from the subject T_1 image to the template T_1 image.

SVR

Imaging patterns of brain development were quantified using a SVR (ε-SVR) algorithm (Smola and Scholkopf 2004). SVR is a supervised learning technique based on the concept of support vector machines (SVM), but generalizes the categorical classification of SVM to predict continuous variables (e.g., age). SVM has many advantages that make it suitable for our high-dimensional pattern recognition problem, such as high generalization performance, as well as easy computation that allows dealing with the curse of dimensionality. In support vector classification, the best separating hyperplane between data samples from 2 different classes is found by maximizing the margin between these 2 classes. The decision function, that is, the classification hyperplane, is fully specified by only the data samples on the margin boundaries, which are called the support vectors. Analogously to SVM, in SVR a regression model that only depends only on a subset of the training data is computed, by ignoring the errors of any training data close to the model prediction within a margin determined by the threshold ε. Thus, one does not care about errors as long as they are less than ε, but will not accept any deviation larger than this (Smola and Scholkopf 2004). SVR attempts to minimize the training error within the ε tolerance, as well as the complexity of the regressor, so as to achieve generalized performance.

BDI

We used the SVR algorithm implemented in LIBSVM (Chang and Lin 2011) to calculate the regression model used for estimating the BDI. As an input to SVR, each subject is represented by a feature vector obtained by concatenating the voxel values from various input image maps, that is, GM, WM, VN RAVENS maps and FA and ADC maps, after automatically masking out the background in each mask. Each feature is independently normalized by scaling the feature values between 0 and 1. In data normalization only training samples are used to calculate scaling parameters, which are also used for scaling the test samples. We did not apply a preliminary feature selection step, as the SVR method is both efficient and computationally feasible for regression problems using very high-dimensional feature vectors as input, but also because patterns of brain change during development are spread throughout the whole brain, and are not localized in specific regions, as is often the case with brain pathologies. The final feature vector, obtained by combining all image maps, contained 1 116 006 features. In order to ensure that derived models would generalize to new individuals, 10-fold cross validation was applied, by each time using 90% of the samples as training data for the regression model, and testing the model on the remaining 10% of the samples. This procedure provides an unbiased estimate of model predictive accuracy and prevents model over-fitting. As the feature dimension is significantly larger than the sample size, a linear kernel was used. The epsilon parameter was set to its default value, $\varepsilon = 0.01$.

Although initially all 5 image maps were used as input, the SVR procedure was repeated using each image type in isolation in order to compare their relative predictive capabilities. Additionally, sex-specific brain development indices were constructed by applying the above procedure separately on males and females. In order to evaluate each sex developmental trajectory relative to the other, the male-trained model was applied to females and vice versa.

Comparison to Cognitive Performance

Finally, we investigated the relationship between each subject's estimated BDI and their cognitive performance. In order to evaluate whether divergent patterns of brain development were associated with cognitive performance, we examined the outliers of the model, that is, those subjects whose predicted age was significantly different from their chronological age. Outliers were identified as subjects who were beyond the 90% confidence interval (CI) band from a linear regression between BDI and chronological age. Outliers having a BDI higher than the prediction interval boundaries are referred to as *advanced* (*advBDI*), and those having a BDI lower than the prediction interval boundaries here are called *delayed* (*delBDI*). Finally, a group of subjects whose chronologic age was well predicted by their imaging data (normal, *normBDI*) was constructed by selecting subjects within a 30% prediction interval of the regression line. The cognitive performances of subjects in the 3 groups were compared using one-way ANOVA between the 3 groups for each cognitive test score for accuracy and speed. Multiple testing correction using false discovery rate (FDR) estimation is applied using the method described in Storey (2002) and adjusted P values (q-values) are reported.

Results

Regional Volumetric Analysis

A global volumetric analysis indicates that age-related differences in volume of GM, WM, and VN were consistent with those reported in the literature (Gogtay et al. 2004; Lenroot and Giedd 2006; Toga et al. 2006): globally, the WM volume increases while the GM volume decreases, as a result of both progressive myelination and regressive pruning processes. Lateral ventricle volume increases linearly with age. Figure 1 shows the age-related differences in cortical GM volume from ages 8 to 22. We observe a consistent decrease in GM volume with age in the whole brain, with region specific patterns of maturation.

BDI

When all image maps were used in combination as input samples, a high estimation accuracy was obtained, with $r = 0.89$ correlation between the BDIs and the chronological ages of subjects (10-fold cross-validated, as described in Materials and methods). The MAE between the estimated and true age was 1.22 years. The scatter plot of the BDIs versus chronological ages of subjects is displayed in Figure 2.

The SVR regression hyperplane that best fits the training data is defined as a weighted combination of all features, where the weight vector, $\vec{w}$, indicates the relative contribution of each feature. Following the approach commonly used in functional MRI analysis using SVM (LaConte et al. 2005), in order to show the contribution of different brain regions in different image modalities we used a direct visualization of the SVR training weight vector. For this visualization we mapped $\vec{w}$ back to initial image domains of each input modality, overlaid each map on the T_1-weighted image of the common template, and showed high values of $\vec{w}$ both in positive and negative directions (Fig. 3). The masking of the weight maps is done using a single threshold value for all image modalities, which corresponds to the 90th percentile of the absolute value of $\vec{w}$.

When the method is applied using each image map independently as input, the prediction accuracy decreased. However the r value was still high, particularly for the ADC ($r = 0.85$, MAE = 1.35), FA ($r = 0.83$, MAE = 1.41), and GM ($r = 0.81$, MAE = 1.52) maps. WM maps obtained a lower r value ($r = 0.76$, MAE = 1.71), and the BDIs obtained using VN maps had relatively much lower correlation with the chronological ages ($r = 0.43$, MAE = 2.71). These results indicate that while

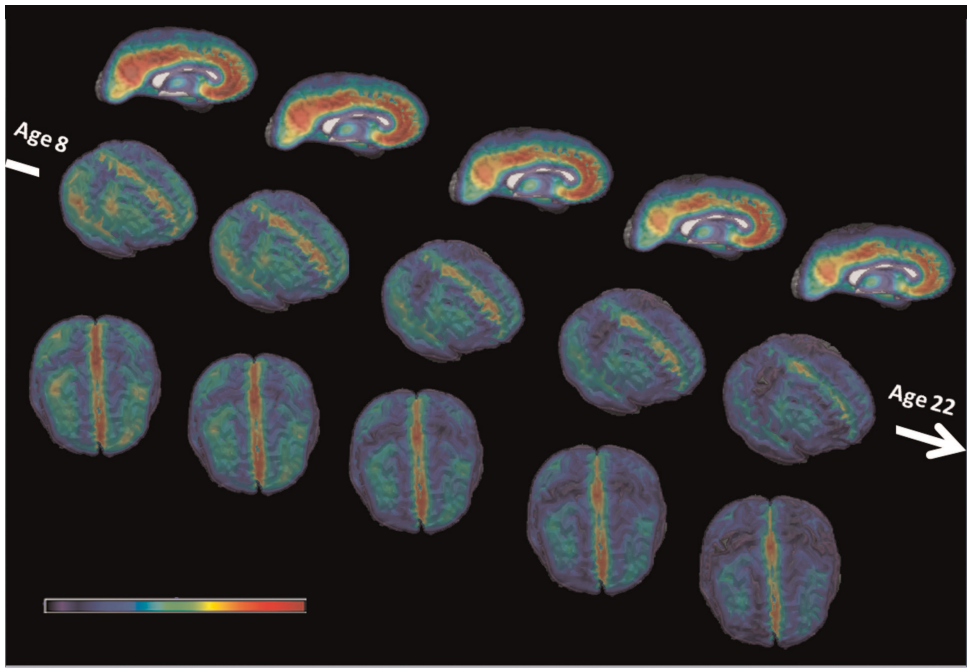

Figure 1. Right mesial, right lateral, and top views of the average GM RAVENS Maps for age groups 8–22. The color map represents lower RAVENS values (i.e., less GM) in blue and higher RAVENS values (i.e., more GM) in red. The GM volume decreases with age in the whole brain, with region specific patterns of maturation.

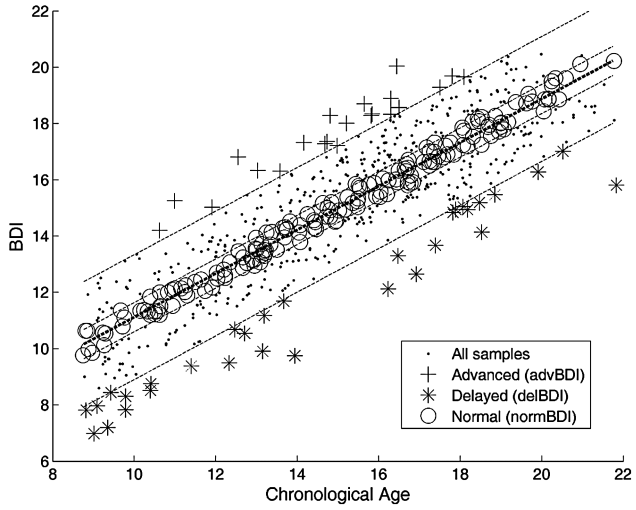

Figure 2. Scatter plot of BDIs versus chronological ages of 621 subjects. The BDIs were calculated through 10-fold cross-validation, using the model trained on the combination of all image maps. The correlation between the chronological age and the BDI is $r = 0.89$. The bold dotted line shows the linear regression line. 90% and 30% prediction intervals are shown with dotted lines. The subjects outside the 90% prediction interval have been labeled as outliers (advanced or delayed brain development). The subjects within the 30% prediction interval have been labeled as normally developed.

single image maps can be used for an accurate estimation of the age, the combination of all maps achieves a higher accuracy in age prediction than the accuracy of each map independently.

We trained sex-specific brain development models, that is, a female model (MF) of age prediction trained using only the female subjects, and a male model (MM) trained using only the male subjects. BDIs of males and females have been calculated separately using images of male and female subjects, respectively, with leave 10% out cross-validation. The prediction accuracy for both sexes were comparable to the accuracy obtained using all subjects together ($r = 0.87$ and MAE = 1.291 for males trained on males, and $r = 0.88$ MAE = 1.264 for females trained on females).

The female and male models have been then applied for predicting the age of the subjects in the other sex. Figure 4 shows the scatter plots of the chronological ages versus BDIs for males and females using the sex-specific models. According to the MM, female subjects have a higher BDI compared with what the MM expected in the early ages, and a lower BDI in ages ranging from 16–21. According to the MF, male subjects have a lower BDI than the female subjects in the early ages, but they close the gap in later ages. To evaluate the significance of sex differences in BDIs obtained using gender-specific models we applied a multivariate regression, with the BDIs as the response variable and age and sex as predictor variables. We found that the BDIs obtained using the female SVR model had a significant group difference for sex ($P = 0.23 \times 10^{-8}$), while the difference was not significant for BDIs obtained using the male SVR model ($P = 0.053$). We also investigated how much of the observed differences could be explained by biological maturation, by including the Tanner stage of each subject into the model as a covariate. After accounting for the effect of biological maturation, the group difference for sex was still significant for BDIs obtained using the female SVR model ($P = 0.001$), while the BDIs from the male SVR model showed no significant sex differences $P = 0.091$.

BDI Versus Cognitive Performance

The subjects in the advance (*advBDI),* delayed (*delBDI*), and normally-developed (*normBDI*) groups were determined

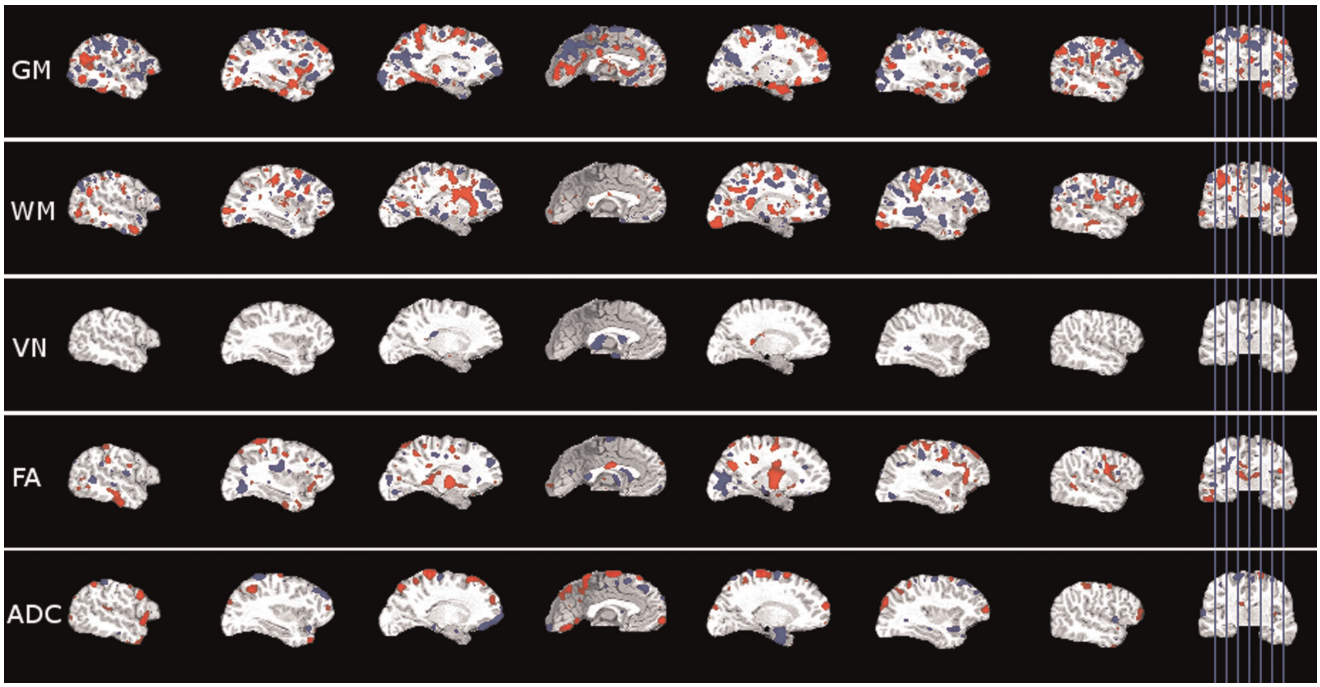

Figure 3. The visualization of the SVR weight vector for the SVR model trained using all image maps from all subjects as input. The highlighted areas in each image map show the brain regions that obtained a high positive (red) or negative (blue) weight.

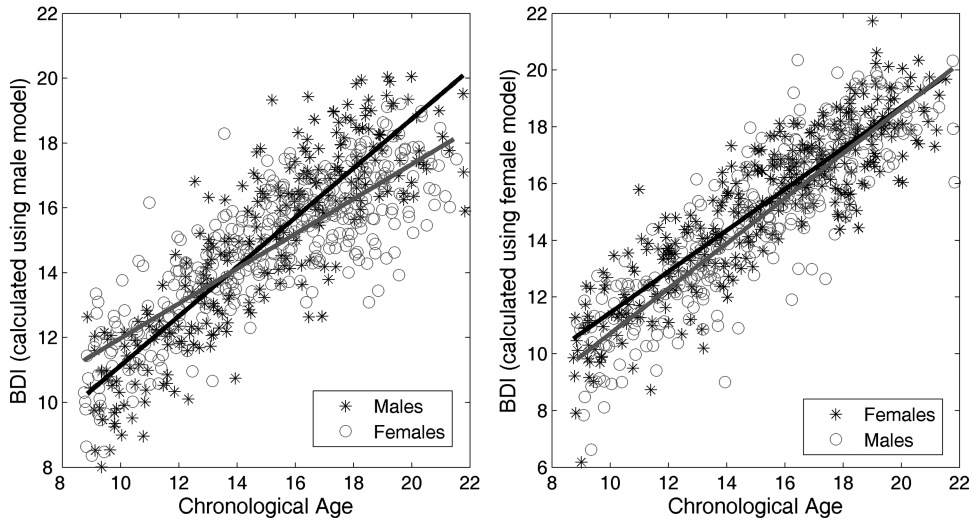

Figure 4. Scatter plot of chronological ages versus BDIs of female and male subjects calculated using sex-specific prediction models. Left: the BDIs for male and female subjects calculated using the model trained on the male subjects only. The linear regression line is shown in black for males and in gray for females. Right: the BDIs for female and male subjects calculated using the model trained on the female subjects only. The linear regression line is shown in black for females and in gray for males. Ten-fold cross validation is used when the model is trained and tested on the same sex.

based on their BDIs calculated using the model trained on all subjects and all image maps (Fig. 2). The number of subjects in each group, the sex and average age of these subjects are given in Table 1. To emphasize the differences between the 3 groups, we visualized the dynamic changes through age for subjects in each group, by creating average GM RAVENS within consecutive age intervals between age 8 and 22 (Fig. 5). We observed a maturational shift between the groups, such that all groups demonstrated similar patterns of maturation, but they occurred earlier in the *advBDI* group and later in the *delBDI* group.

We compared the cognitive performance of the subjects in the 3 groups, by applying a one-way ANOVA between groups for each test score. FDR corrected P values (q values) for accuracy and speed scores in each test are given in Table 2. Notably, we observed significant group differences in speed, the most significant effect being observed in motor speed (MOT) test. All 3 tests in memory domain had significant

q value for speed, while the q values for tests in cognition domain were not significant. In accuracy scores, only the abstraction and mental flexibility (ABF) test in the executive domain had significant group differences. Figure 6 shows the average scores of subjects in each group for each test, normalized by the scores of the normal group for a better visualization of group differences.

In order to assess the possibility that these results were driven largely or entirely by the DTI variables we repeated the same analysis after grouping the subjects into the advanced, delayed, and normal groups based on the BDIs calculated using only the ADC, and ADC and TR together. In both cases the groups displayed differences consistent with the previous findings, with advanced group showing a higher performance in speed, however, the group differences were not significant after FDR correction (i.e., $q > 0.05$).

Table 1
Summary statistics of subjects in advanced, delayed, and normal groups

	N	Male	Female	Age	MAE
advBDI	22	12	10	14.89 ± 2.10	2.81
delBDI	31	15	16	14.39 ± 4.00	2.78
normBDI	165	72	93	14.92 ± 3.25	0.63

Discussion

The applied framework utilized advanced image analysis methodology to derive an index of brain maturation from structural MR images using T_1 and DTI protocols. A multivariate regression method using SVM was applied to map the very high-dimensional feature vector consisting of voxel values from T_1 and DTI processed images into an index of brain maturation. The developmental trajectory of the brain has been successfully captured by this model, as reflected by a cross-validated correlation coefficient between chronologic age and the BDI of $r = 0.89$.

Both tissue density maps for GM, WM, and VN derived from T_1-weigthed images, and FA and ADC maps from DTI images were used in combination as imaging data. While the models using single image maps were also successful in predicting age, the highest accuracy was obtained by the combination of voxel-wise features from all image maps. These quantitative

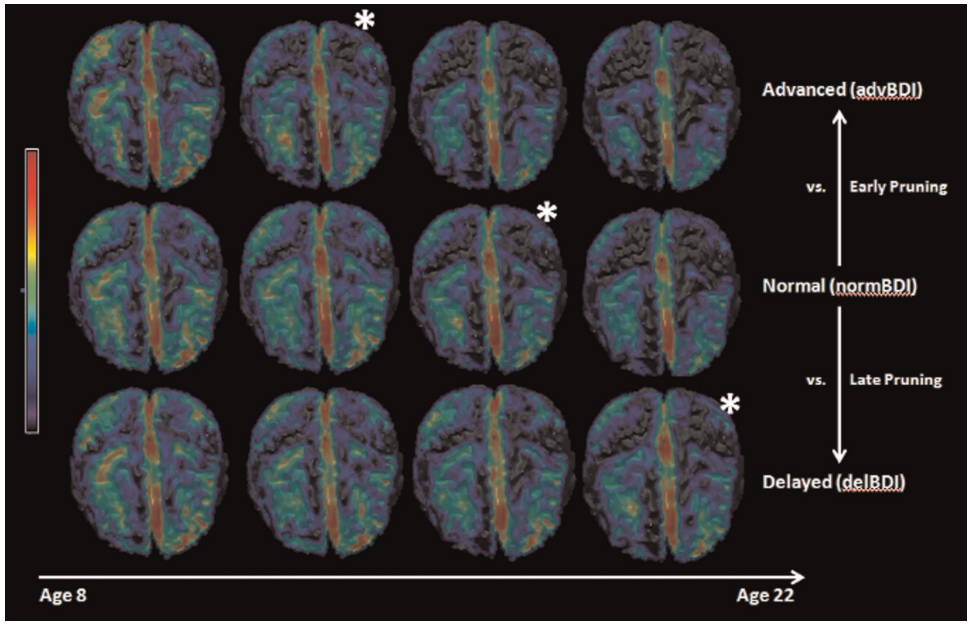

Figure 5. Top views of average GM RAVENS Maps in different age groups for the advanced, delayed, and normal subjects. The color map represents lower RAVENS values (i.e., less GM) in blue and higher RAVENS values (i.e., more GM) in red. A consistent developmental pattern is observed for all groups similar to that shown in Figure 1. However a shift can be observed between the 3 groups, where the GM decrease happens earlier in the advanced group, and later in the delayed group, compared with normal group. The * has been used to show the correspondences, as an indicator of this developmental shift.

Table 2
Group comparisons with ANOVA for accuracy and speed scores in cognitive domains (please refer to Materials and methods for abbreviations used in cognitive test names)

Domain	Executive			Memory			Cognition			Social cognition			Praxis speed	
Test	ABF	ATT	WM	VMEM	FMEM	SMEM	LAN	NVR	SPA	EMI	EMD	AGD	MOT	SM
q														
Accuracy	**0.029**	0.145	0.133	0.347	0.146	0.307	0.109	0.069	0.335	0.347	0.223	0.150		
Speed	0.227	**0.020**	0.063	**0.008**	**0.005**	**0.031**	0.094	0.096	0.227	**0.044**	0.139	0.134	**0.004**	**0.033**

Note: A one-way ANOVA is applied on each cognitive test to compare scores of the subjects in advBDI, delBDI, and normBDI groups. Multiple testing correction using FDR estimation is applied and adjusted *P* values (*q*-values) are reported. Significant ($q < 0.05$) values are indicated in bold font.

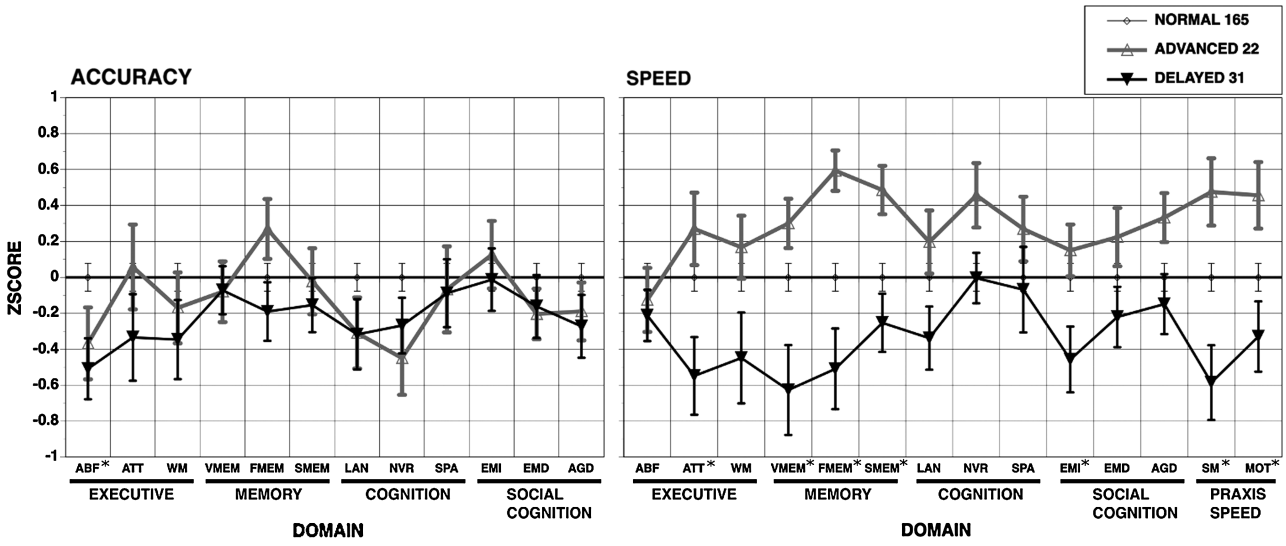

Figure 6. Mean(±SEM) scores in each cognitive domain for subjects in normal, advanced, and delayed groups. The scores in each cognitive domain were normalized to those whose BDI age is within 30% CI of chronological age (NORMAL), such that the normal group has zero mean and SD equal to one. The cognitive domains with significant group differences are marked with *. See domain abbreviations in Materials and methods.

results point to the contribution of complementary information from each of these different maps, but also to a certain redundancy in their information content. When the method was applied in each sex independently, a comparable accuracy was obtained, showing that the method successfully captured sex-specific patterns of brain maturation. Sex differences in applying the model learned from one sex on another support multiple studies suggesting earlier maturation in females (De Bellis et al. 2001; Lenroot et al. 2007). Specifically, as predicted, BDI scores based on males overestimated chronological age in females, especially in the younger age groups, while female-based BDI scores underestimated male chronological ages, again most noticeably in the younger age groups.

In order to show the contribution of different brain regions in different image modalities we used a direct visualization of the SVR training weight vector. We should note that, while being informative on the relative contribution of specific brain regions to the regression hyperplane, the $\vec{w}$ maps do not provide a measure that could be directly used to compare different image maps. As a future work, we plan to apply multikernel learning (Gonen and Alpaydin 2011), a recent technique that is used for combining high-dimensional data from different sources in a more structured way within the SVM framework, which will give us the possibility to compare the overall contribution of different image maps.

In adolescence, in parallel to structural brain changes, core cognitive processes continue to develop and mature. As noted by Paus (2005), quantitative morphometric features can be used as a "dependent" variable in studies of brain–behavior relationships. Recent findings have shown significant correlations between regional patterns of structural brain change and cognitive development (Gogtay et al. 2004; Sowell et al. 2004; Blakemore and Choudhury 2006; Shaw et al. 2006; Tamnes et al. 2010a, 2010b). Using longitudinal scans Shaw et al. (2006) demonstrated that intelligence scores are associated with the trajectory of cortical development in childhood and adolescence. Gogtay et al. (2004) reported accelerated maturation of frontal lobe during adolescence and related it to increased effectiveness of executive functions. Reviewing 37 neuroimaging studies, Jung and Haier (2007) reported a striking consensus on findings that relate individual differences in intelligence test scores to variations in brain structure and function. In light of these findings, we hypothesized that multimodal, multivariate patterns of brain maturation would relate to individual differences in cognition. Accordingly, we investigated the relationship between cognition, as measured by cognitive test performance in several domains, and the difference of the estimated BDI from the chronological age.

The neurocognitive effects indicate greater maturational effects on speed than accuracy, which is consistent with multiple studies on age-related changes in performance across the lifespan (Kail 2007; Coyle et al. 2011). A cross-sectional study of cognitive maturation in healthy subjects ages 8–30 (Luna et al. 2004) indicated maturation of processing speed through late childhood and into adolescence. Notably, the developmental increases in speed of information processing reflected a distinct process from the development of accuracy, which also matures albeit at a slower slope than speed (Gur et al. 2012) during adolescence. The improved speed of performance could be attributed to increased efficiency in neuronal organization and communication through myelination and pruning processes. The multivariate approach is well suited for better capturing such effects that span over brain regions.

Contrary to our expectations, both the advanced and delayed groups performed less accurately on the abstraction and mental flexibility domain, as well as on the complex cognition domains of language and nonverbal reasoning. It appears that advanced compared with delayed maturation effects are exclusive for speed of performance, whereas both can adversely affect performance on tasks that require more extensive cortical resources. The path to poorer accuracy could be different for the 2 groups. Precocious maturers may over-apply speed that can hinder accuracy on tasks that require reflection and computation, while delayed maturers may lack the cerebral resources

for accurate performance and are hence both slow and inaccurate. Future studies can examine regional correlations with performance to elucidate the issue.

The BDI could have important clinical utility. In the first place, it could be used for creating "brain growth charts" similar to those used by pediatricians to follow a child"s growth. By observing BDIs of a large number of healthy children over time, such tools could be used for following deviations or delays from normal brain development. Luna and Sweeney (2001) emphasized the need for neurobehavioral and neuroimaging studies characterizing normal development before examining at-risk or clinical populations, referring specifically to elucidation of dysmaturation processes in schizophrenia. It is noteworthy that Bachman et al. (2012) reported that adolescent-onset psychosis patients fail to show normal age-related increases in processing speed, which in turn predicts poorer functional outcomes.

In this paper we had a relatively limited but focused scope that basically aimed to investigate the relationship between the cognitive development and structural brain changes in maturation. The PNC data, with multimodal MRI images, large sample size and a well-designed cognitive battery, provided a very good opportunity to work on this problem. Importantly, a second potential clinical aim of our work would be to provide early biomarkers of pathologic deviations from the normal trajectory of brain development. A future direction of our research will be to focus specifically on subjects with prominent psychopathology, as diagnosed by clinical assessment, extending this study to other datasets. This would permit examining differences in brain development trajectories in specific disorders compared with a normative population, and provide a tool for early identification of neuropsychiatric pathology.

Establishing the PNC as a publicly available resource for the study of brain development was one of the principal aims of the initiative. Accordingly, all nonidentifying data acquired as part of the PNC will be made public and freely available to qualified investigators. Details on data sharing are available in the article that describes the study design (Satterthwaite et al. 2013).

Funding

This work was supported by NIH grant NIA-R01-14971 and RC2 grants from the National Institute of Mental Health (MH089983 and MH089924) as well as T32 MH019112. Dr Satterthwaite was supported by NIMH K23MH098130 and the Marc Rapport Family Investigator grant through the Brain and Behavior Research Foundation.

Notes

The authors thank the acquisition team, including James Loughead, Karthik Prabhakaran, Ryan Hopson, Jeff Valdez, Marisa Riley, Jack Keefe, Raphael Gerraty, Nicholas DeLeo, and Elliot Yodh. *Conflict of Interest*: None declared.

References

Asato MR, Terwilliger R, Woo J, Luna B. 2010. White matter development in adolescence: a DTI study. Cereb Cortex. 20:2122–2131.

Ashtari M, Cervellione KL, Hasan KM, Wu J, McIlree C, Kester H, Ardekani BA, Roofeh D, Szeszko PR, Kumra S. 2007. White matter development during late adolescence in healthy males: a cross-sectional diffusion tensor imaging study. NeuroImage. 35:501–510.

Bachman P, Niendam TA, Jalbrzikowkski M, Park CY, Daley M, Cannon TD, Bearden CE. 2012. Processing speed and neurodevelopment in adolescent-onset psychosis: cognitive slowing predicts social function. J Abnorm Child Psychol. 40:645–654.

Ball WS, Byars AW, Schapiro M, Bommer W, Carr A, German A, Dunn S, Rivkin MJ, Waber D, Mulkern R et al. 2012. Total and regional brain volumes in a population-based normative sample from 4 to 18 years: the NIH MRI study of normal brain development. Cereb Cortex. 22:1–12.

Barnea-Goraly N, Menon V, Eckert M, Tamm L, Bammer R, Karchemskiy A, Dant CC, Reiss AL. 2005. White matter development during childhood and adolescence: a cross-sectional diffusion tensor imaging study. Cereb Cortex. 15:1848–1854.

Beresford TP, Arciniegas DB, Alfers J, Clapp L, Martin B, Du Y, Liu D, Shen D, Davatzikos C. 2006. Hippocampus volume loss due to chronic heavy drinking. Alcohol Clin Exp Res. 30:1866–1870.

Blakemore SJ, Choudhury S. 2006. Development of the adolescent brain: implications for executive function and social cognition. J Child Psychol Psychiatry. 47:296–312.

Brown TT, Kuperman JM, Chung Y, Erhart M, McCabe C, Hagler DJ, Venkatraman VK, Akshoomoff N, Amaral DG, Bloss CS et al. 2012. Neuroanatomical assessment of biological maturity. Curr Biol. 22:1693–1698.

Bunge Silvia A, Whitaker Kirstie J. 2012. Brain imaging: your brain scan doesn't lie about your age. Curr Biol. 22:R800–R801.

Chang C-C, Lin C-J. 2011. LIBSVM: a library for support vector machines. ACM Trans. Intell. Syst Technol. 2:1–27.

Coyle TR, Pillow DR, Snyder AC, Kochunov P. 2011. Processing speed mediates the development of general intelligence (g) in adolescence. Psychol Sci. 22:1265–1269.

Davatzikos C, Genc A, Xu D, Resnick SM. 2001. Voxel-based morphometry using the RAVENS maps: methods and validation using simulated longitudinal atrophy. NeuroImage. 14:1361–1369.

De Bellis MD, Keshavan MS, Beers SR, Hall J, Frustaci K, Masalehdan A, Noll J, Boring AM. 2001. Sex differences in brain maturation during childhood and adolescence. Cereb Cortex. 11:552–557.

Dosenbach NUF, Nardos B, Cohen AL, Fair DA, Power JD, Church JA, Nelson SM, Wig GS, Vogel AC, Lessov-Schlaggar CN et al. 2010. Prediction of individual brain maturity using fMRI. Science. 329:1358–1361.

Driscoll I, Davatzikos C, An Y, Wu X, Shen D, Kraut M, Resnick SM. 2009. Longitudinal pattern of regional brain volume change differentiates normal aging from MCI. Neurology. 72:1906–1913.

Franke K, Luders E, May A, Wilke M, Gaser C. 2012. Brain maturation: predicting individual BrainAGE in children and adolescents using structural MRI. NeuroImage. 63:1305–1312.

Franke K, Ziegler G, Kloppel S, Gaser C. 2010. Estimating the age of healthy subjects from T1-weighted MRI scans using kernel methods: exploring the influence of various parameters. NeuroImage. 50:883–892.

Giedd JN, Blumenthal J, Jeffries NO, Castellanos FX, Liu H, Zijdenbos A, Paus T, Evans AC, Rapoport JL. 1999. Brain development during childhood and adolescence: a longitudinal MRI study. Nat Neurosci. 2:861–863.

Giedd JN, Rapoport JL. 2010. Structural MRI of pediatric brain development: what have we learned and where are we going? Neuron. 67:728–734.

Gogtay N, Giedd JN, Lusk L, Hayashi KM, Greenstein D, Vaituzis AC, Nugent III TF, Herman DH, Clasen LS, Toga AW et al. 2004. Dynamic mapping of human cortical development during childhood through early adulthood. Proc Natl Acad Sci. 101:8174–8179.

Goldszal AF, Davatzikos C, Pham DL, Yan MX, Bryan RN, Resnick SM. 1998. An image-processing system for qualitative and quantitative volumetric analysis of brain images. J Comput Assist Tomogr. 22:827–837.

Gonen M, Alpaydin E. 2011. Multiple kernel learning algorithms. J Mach Learn Res. 12:2211–2268.

Gur R, Davatzikos C, Shen D, Wu X, Fan Y, Hughett P, Turetsky B, Gur R. 2006. Whole-brain deformation based morphometry MRI study of schizophrenia. Schizophr Bull. 31:408–408.

Gur RC, Richard J, Calkins ME, Chiavacci R, Hansen JA, Bilker WB, Loughead J, Connolly JJ, Qiu H, Mentch FD et al. 2012. Age group and sex differences in performance on a computerized neurocognitive battery in children age 8–21. Neuropsychology. 26:251–265.

Gur RC, Richard J, Hughett P, Calkins ME, Macy L, Bilker WB, Brensinger C, Gur RE. 2010. A cognitive neuroscience-based computerized battery for efficient measurement of individual differences: standardization and initial construct validation. J Neurosci Methods. 187:254–262.

Insel TR. 2009. Translating scientific opportunity into public health impact: a strategic plan for research on mental illness. Arch Gen Psychiatry. 66:128–133.

Jung RE, Haier RJ. 2007. The parieto-frontal integration theory (p-fit) of intelligence: converging neuroimaging evidence. Behav Brain Sci. 30:135–154.

Kail RV. 2007. Longitudinal evidence that increases in processing speed and working memory enhance children's reasoning. Psychol Sci. 18:312–313.

LaConte S, Strother S, Cherkassky V, Anderson J, Hu X. 2005. Support vector machines for temporal classification of block design fMRI data. NeuroImage. 26:317–329.

Lebel C, Beaulieu C. 2011. Longitudinal development of human brain wiring continues from childhood into adulthood. J Neurosci. 31:10937–10947.

Le Bihan D, Mangin JF, Poupon C, Clark CA, Pappata S, Molko N, Chabriat H. 2001. Diffusion tensor imaging: concepts and applications. J Magn Reson Imaging. 13:534–546.

Lenroot RK, Giedd JN. 2006. Brain development in children and adolescents: insights from anatomical magnetic resonance imaging. Neurosci Biobehav Rev. 30:718–729.

Lenroot RK, Greenstein D, Gogtay N, Wallace GL, Clasen LS, Blumenthal JD, Wells EM, Lerch JP, Zijdenbos AP, Evans AC et al. 2007. Sexual dimorphism of brain developmental trajectories during childhood and adolescence. NeuroImage. 36:1965–1973.

Luna B, Garver KE, Urban TA, Lazar NA, Sweeney JA. 2004. Maturation of cognitive processes from late childhood to adulthood. Child Dev. 75:1357–1372.

Luna B, Sweeney JA. 2001. Studies of brain and cognitive maturation through childhood and adolescence: a strategy for testing neurodevelopmental hypotheses. Schizophr Bull. 27:443–455.

Mukherjee P, Miller JH, Shimony JS, Conturo TE, Lee BCP, Almli CR, McKinstry RC. 2001. Normal brain maturation during childhood: developmental trends characterized with diffusion-tensor MR imaging1. Radiology. 221:349–358.

Nellhaus G. 1968. Head circumference from birth to eighteen years. Practical composite international and interracial graphs. Pediatrics. 41:106–114.

Ou Y, Sotiras A, Paragios N, Davatzikos C. 2011. DRAMMS: deformable registration via attribute matching and mutual-saliency weighting. Med Image Anal. 15:622–639.

Paus T. 2005. Mapping brain maturation and cognitive development during adolescence. Trends Cogn Sci. 9:60–68.

Paus T, Keshavan M, Giedd JN. 2008. Why do many psychiatric disorders emerge during adolescence? Nat Rev Neurosci. 9:947–957.

Resnick SM, Goldszal A, Davatzikos C, Golski S, Kraut MA, Metter EJ, Bryan RN, Zonderman AB. 2000. One-year age changes in MRI brain volumes in older adults. Cereb Cortex. 10:464–472.

Satterthwaite TD, Elliott MA, Ruparel K, Loughead J, Prabhakaran K, Calkins ME, Hopson R, Jackson C, Keefe J, Riley M et al. 2013. Neuroimaging of the Philadelphia Neurodevelopmental Cohort. NeuroImage. In Press.

Shaw P, Greenstein D, Lerch J, Clasen L, Lenroot R, Gogtay N, Evans A, Rapoport J, Giedd J. 2006. Intellectual ability and cortical development in children and adolescents. Nature. 440:676–679.

Silk TJ, Wood AG. 2011. Lessons about neurodevelopment from anatomical magnetic resonance imaging. J Dev Behav Pediatr. 32:158–168.

Smola AJ, Scholkopf B. 2004. A tutorial on support vector regression. Stat Comput. 14:199–222.

Sowell ER, Thompson PM, Leonard CM, Welcome SE, Kan E, Toga AW. 2004. Longitudinal mapping of cortical thickness and brain growth in normal children. J Neurosci. 24:8223–8231.

Storey JD. 2002. A direct approach to false discovery rates. J R Stat Soc Ser B. 64:479–498.

Tamnes CK, Ostby Y, Fjell AM, Westlye LT, Due-Tonnessen P, Walhovd KB. 2010a. Brain maturation in adolescence and young adulthood: regional age-related changes in cortical thickness and white matter volume and microstructure. Cereb Cortex. 20:534–548.

Tamnes CK, Ostby Y, Walhovd KB, Westlye LT, Due-Tonnessen P, Fjell AM. 2010b. Neuroanatomical correlates of executive functions in children and adolescents: a magnetic resonance imaging (MRI) study of cortical thickness. Neuropsychologia. 48:2496–2508.

Toga AW, Thompson PM, Sowell ER. 2006. Mapping brain maturation. Trends Neurosci. 29:148–159.